Energy Conversion and Management: X 27 (2025) 101167

Contents lists available at ScienceDirect

Energy Conversion and Management: X

journal homepage: www.sciencedirect.com/journal/energy-conversion-and-management-x

Low-carbon heating solutions using road thermal collectors and seasonal energy storage in mediterranean climates☆

Stefania Guarino *, Alessandro Buscemi, Marina Bonomolo, Marco Beccali, Valerio Lo Brano

Department of Engineering, University of Palermo, Italy

ARTICLE INFO

Keywords:
Heat-Harvesting Systems
Cool Pavement Technology
Road Thermal Collectors (RTCs)
Seasonal Thermal Energy Storage (STES)
Borehole Thermal Energy Storage (BTES)
Sustainable Heating Systems
Solar-Assisted Heat Pump Systems

ABSTRACT

The building sector accounts for 40% of final energy consumption and 36% of energy-related greenhouse gas emissions in Europe, positioning it as a critical target for decarbonisation under the European Green Deal. Road Thermal Collectors (RTCs), a type of heat-harvesting system, utilize urban surfaces like roads to capture solar energy for thermal applications. When combined with Borehole Thermal Energy Storage (BTES) and water-to-water heat pumps, RTCs provide a multifunctional, low-carbon heating solution while also mitigating urban heat island effects. This study investigates an RTC-BTES hybrid heating system in a school building in southern Italy, where t—he Mediterranean climate poses unique challenges and opportunities for seasonal thermal energy storage. The system's performance is assessed through dynamic simulations using TRNSYS software, with RTC models validated against experimental data from the University of Palermo. A typical school with an annual heating demand of 166 MWh was analysed, comparing the performance of the proposed integrated heating system with one using conventional gas boilers. The results demonstrate that the integrated system significantly reduces primary energy consumption and CO_2 emissions, offering a scalable and sustainable alternative to fossil fuel-based heating, advancing low-carbon solutions for non-residential buildings.

Introduction

The building sector is a major driver of global energy consumption and carbon emissions, accounting for 30 % of global energy use and 37 % of energy-related CO_2 emissions in 2023, equivalent to approximately 9.5 gigatonnes of CO_2 per year [1,2]. These figures highlight the sector's dual role as a significant contributor to climate change and a key target for decarbonisation efforts. Transitioning the building sector to sustainable energy systems remains a significant challenge, requiring the adoption of integrated renewable energy systems, advanced thermal storage technologies, and innovative solutions to close the gap between energy supply and demand [3]. To address the environmental impact of buildings, a comprehensive strategy is essential, combining energy efficiency improvements, materials innovation and the adoption of low-carbon technologies [4,5]. While progress has been made in electrification and the use of renewable energy in buildings, fossil fuels continue to dominate in many regions, slowing the energy transition [2]. Achieving global climate targets requires an accelerated decarbonization of both building operations and the construction supply chain to reduce the sector's long-term environmental impact.

This shift is being driven by efforts to decarbonize electricity, expand district heating and cooling systems, and integrate renewable energy sources such as solar thermal and geothermal energy [6], further emphasising the central role of the building sector in promoting sustainable energy systems [7]. In Europe, where buildings account for 40 % of final energy consumption and 36 % of energy-related greenhouse gas emissions, the European Green Deal sets ambitious goals to improve energy efficiency and sustainability in the building sector. With a target to reduce greenhouse gas emissions by 55 % by 2030 and achieve climate neutrality by 2050, this initiative places a strong emphasis on integrating renewable energy and accelerating building retrofitting across the EU [8].

Beyond decarbonization, the challenges of global warming and urbanization further complicate the building sector's transformation. The Urban Heat Island (UHI) effect, characterized by elevated temperatures in dense urban areas compared to their rural surroundings, exacerbates energy demands for cooling and heating, worsens air quality, and reduces thermal comfort [9,10]. Pavements and road surfaces play a significant role in this phenomenon, absorbing and storing solar radiation,

☆ This article is part of a special issue entitled: 'SDEWES 2024_ECMX' published in Energy Conversion and Management: X.

* Corresponding author at: Department of Engineering, University of Palermo, Italy.
E-mail addresses: stefania.guarino@unipa.it (S. Guarino), alessandro.buscemi@unipa.it (A. Buscemi), marina.bonomolo@unipa.it (M. Bonomolo), marco.beccali@unipa.it (M. Beccali), valerio.lobrano@unipa.it (V. Lo Brano).

https://doi.org/10.1016/j.ecmx.2025.101167
Received 14 January 2025; Received in revised form 10 June 2025; Accepted 24 July 2025
Available online 26 July 2025

Nomenclature

Symbols

C_{eq}	equivalent CO_2 emissions avoided in one year [$kgCO_{2\text{-}eq}$/y]
C_c	COP degradation factor of the heat pump [-]
$c_{p,f}$	specific heat of fluid [J/(kg•K)]
$C_{p,s}$	heat capacity of the soil [J/K]
COP_{FL}	COP of the heat pump under full load conditions [-]
COP_{PL}	COP of the heat pump under partial load conditions [-]
E_{boiler}	annual thermal energy output of the gas boiler [MWh/y]
$E_{e,plant}$	annual electricity consumption of the plant [MWh/y]
$E_{ev,HP}$	annual thermal energy delivered to the heat pump evaporator [MWh/y]
E_{load}	school's thermal energy requirements for space heating [MWh/y]
$E_{i,BTES}$	cumulative energy input to the BTES [MWh]
$E_{o,BTES}$	cumulative energy output from the BTES [MWh]
E_{sun}	solar energy collected by the RTC opening surface [MWh/y]
$E_{th,RTC}$	thermal energy produced by the RTC [MWh/y]
$E_{th,HP}$	thermal energy supplied to the school by the heat pump system [MWh/y]
f_{HP}	fraction of the school's heat demand met by the heat pump [-]
f_{sav}	fractional energy savings [%]
H_b	length of boreholes
I_h	global irradiation on the horizontal surface [kWh/m^2]
$\dot{m}_{f,HP}$	mass flow rate of the fluid [kg/s]
$n_{b,h}$	number of boreholes connected in parallel
$n_{b,s}$	number of boreholes connected in series
$n_{b,t}$	total number of boreholes
$\dot{Q}_{actual}$	actual operational thermal load of the heat pump [kW]
$\dot{Q}_{ev}$	thermal input power of the heat pump evaporator [kW]
$\dot{Q}_H^{max}$	maximum heat capacity of the heat pump [kW]
r_b	radius of the borehole [m]
R_p	thermal resistance of the borehole [K/W]
$r_{p,i}$	inner radius of the pipes [m]
$r_{p,o}$	outer radius of the pipes [m]
s_b	spacing between the concentric rings along which boreholes are distributed [m]
$T_{ave,BTES}$	average temperature of the storage volume
$T_{ev,i}$	temperature of the fluid entering the evaporator [°C]
$T_{ev,o}$	temperature of the fluid exiting the evaporator [°C]
$T_{i,BTES}$	temperature of the heat transfer fluid entering the BTES [°C]
$T_{o,BTES}$	temperature of the heat transfer fluid exiting the BTES [°C]
$T_{s,0}$	undisturbed soil temperature [°C]
V_{BTES}	volume of geothermal storage [m^3]
x_c	half shank spacing between the U-legs [m]

Greek letters

ε_e	primary energy conversion factors for the electricity [kWh_p/kWh_e]
ε_{fuel}	primary energy conversion factors for the natural gas [kWh_p/kWh_e]
η_{boiler}	efficiency of the gas boiler [%]
η_{RTC}	efficiency of the RTC [%]
$\eta_{storage}$	efficiency of the storage system [%]
λ_g	thermal conductivities of the grout [W/(m•K)]
λ_p	thermal conductivity of the pipe [W/(m•K)]
λ_s	thermal conductivities of the soil [W/(m•K)]
$\mu_{\substack{e,fuel \\ mix}}$	emission factor for grid-supplied electricity [$kgCO_{2\text{-}eq}$/kWh_e]
$\mu_{\substack{natural \\ gas}}$	emission factor for thermal energy from natural gas [$kgCO_{2\text{-}eq}/kWh_{th}$]

Acronyms

BTES	Borehole Thermal Energy Storage
CHP	Combined Heat and Power
CO_2	Carbon Dioxide
COP	Coefficient of Performance
DST	Duct Ground Heat Storage Model
FEM	Finite Element Method
HDD	Heating Degree Days
HP	Heat Pump
HTF	Heat Transfer Fluid
PER	Primary Energy Ratio
PLF	Partial Load Factor
PLR	Partial Load Ratio
RER	Renewable Energy Ratio
RTC	Road Thermal Collector
SCOP	Seasonal Coefficient of Performance
SHP	Solar and Heat Pump
STES	Seasonal Thermal Energy Storage
TRNSYS	Transient System Simulation Tool
UHI	Urban Heat Island

which is then released as heat and amplifies local temperature rises [11]. Addressing the UHI effect calls for sustainable urban design strategies, including the implementation of cool pavements—innovative surfaces designed to reduce temperatures and improve thermal comfort. These solutions can be categorized as reflective, evaporative, or heat-harvesting systems [12]. Among heat-harvesting systems, Road Thermal Collectors (RTCs) stand out for their dual functionality: they reduce surface temperatures by capturing the solar energy absorbed by the asphalt and reuse this energy for practical thermal applications through collectors embedded beneath the pavement [13,14]. Additionally, RTCs can be employed to heat road surfaces in colder climates, preventing freezing and improving safety during winter months [15]. This dual benefit supports decarbonization efforts by integrating renewable energy sources for space heating and hot water production, while simultaneously addressing urban climate challenges.

In the buildings, gas boilers and furnaces currently dominate the technology options for space heating and hot water production [16]. Conversely, heat pumps are becoming the leading technology as a cleaner alternative to meet sustainability goals [17]. These pumps, especially effective when powered by renewable electricity, transfer heat and surpass the efficiency of traditional systems. Types of heat pumps for buildings include air-to-water, air-to-air, and ground source, all of which can be complemented by solar thermal systems [18]. In the latter case, it is crucial to integrate the solar thermal system, designed for heat production, with seasonal thermal energy storage. This combination significantly improves the annual efficiency of a heating system that utilizes renewable energy, addressing the issue of mismatched timing between heat production and demand periods [19].

Within the realm of Seasonal Thermal Energy Storage systems (STESs), Borehole Thermal Energy Storage (BTES) systems are emerging as a viable economic option. These systems utilize soil for the sensible storage of heat and are increasingly seen as a potential alternative to large cogeneration plants, aiming to lower greenhouse gas emissions in district heating systems [20]. BTES systems can efficiently store heat from various sources, including different types of solar collectors, industrial waste heat, or the output of combined power and heat (CHP)

systems.

RTCs offer a multifunctional solution, particularly when coupled with seasonal thermal storage systems like Borehole Thermal Energy Storage (BTES) [20–22]. Recent advancements in hybrid renewable energy systems underscore the effectiveness of integrating solar thermal and geothermal technologies with advanced storage solutions [23]. These systems enable the storage of excess heat during warmer months for use during colder periods, effectively addressing the seasonal mismatch between energy supply and demand [19,22,24]. By utilizing existing urban infrastructure, RTCs avoid the space constraints typically associated with flat-plate solar collectors, making them an ideal choice for high-density urban areas. Unlike conventional flat-plate solar collectors that require dedicated space, RTCs utilize existing urban surfaces, such as roads and sports fields, without compromising their primary functionality. This multifunctional approach makes RTCs particularly advantageous in space-constrained urban areas.

By integrating RTCs with borehole thermal energy storage systems and water-to-water heat pumps, it would be possible to harness solar thermal energy efficiently, store it seasonally, and use it later to meet the winter heating demand of buildings. This approach could be particularly well-suited to the Mediterranean climate, characterized by mild winters and hot summers, where the heating demand is concentrated during a relatively short period, while solar energy availability peaks in the summer months [25,26].

In a previous study, Panno et al. demonstrated the feasibility and performance of a solar-assisted heating system incorporating flat-plate solar collectors and a geothermal storage system for a school building in the Mediterranean climate of southern Italy. The energy captured and stored in the BTES system was utilized by two heat pumps to cover part of the thermal loads of the school, achieving approximately 50 % energy savings compared to a conventional system based solely on gas boilers [27]. Building upon this foundational work, the current study explores the replacement of flat-plate collectors with RTCs for heat production, aiming to evaluate their performance and applicability in similar contexts.

This research introduces an innovative hybrid heating system that integrates RTCs with a BTES system and two water-to-water heat pumps. The study seeks to address existing knowledge gaps by evaluating the technical feasibility, energy efficiency, and environmental impact of this novel configuration within a typical school building located in the south of Italy – a region that presents unique challenges and opportunities for sustainable heating in educational facilities. Schools represent an ideal testbed for these technologies due to their consistent heating demands and the potential replicability of results across other non-residential buildings, such as offices, hospitals, and sports facilities. In this study, a typical school building characterized by a heated volume of 14500 m^3 and an annual energy demand for space heating of about 166 MWh was considered. The analysed plant layout includes two water-water heat pumps with a total heating capacity of 476 kW, an RTC solar field covering around 1000 m^2, and a BTES with 48 double-U probes 25 m deep. Additionally, it was assumed that a conventional heating system would be maintained as a backup, based on gas boilers with a nominal heat capacity of 800 kW. All simulations were conducted in a dynamic state using TRNSYS software – Transient System Simulation Tool – and the model for the road solar collector was developed and calibrated using experimental data collected during a measurement campaign of an actual RTC system realized at the University of Palermo campus [28].

Furthermore, the study showcases the advantages of these systems in reducing primary energy consumption and avoiding equivalent CO_2 emissions, contributing to the broader goal of transitioning towards sustainable, low-carbon heating solutions in non-residential buildings. The environmental benefits, in terms of CO_2 emissions avoided, were assessed by comparing the proposed integrated system with a conventional heating system based solely on gas boilers. This comparison underscores the importance of adopting renewable energy technologies and innovative thermal storage solutions in meeting the heating demands of educational buildings, aligning with environmental sustainability goals.

Although the thermal conversion efficiency of RTCs is relatively modest, their integration into existing urban infrastructure enables multifunctional use of surfaces that would otherwise remain passive. This approach allows for energy harvesting without additional land requirements or visual impact, making RTCs particularly suitable for densely populated urban areas [29]. The present study focuses on evaluating the energy and environmental benefits of the proposed RTC–BTES–HP configuration, while economic analysis is left to future developments.

The paper is organized into the following sections: Section 1 describes the proposed plant layout, describes the numerical models developed to simulate the system's operation, and defines the metrics used for both energy performance analysis and the evaluation of avoided carbon dioxide emissions. Section 2 presents and discusses the results, and finally, Section 3 outlines the conclusions, highlighting the potential and limitations of the proposed approach.

Novelties and contributions of the work

This study presents a novel approach to sustainable heating in educational buildings by integrating Road Thermal Collectors with Borehole Thermal Energy Storage and water-to-water heat pumps. BTES and heat pump systems are established technologies in renewable heating; however, integrating RTCs as a solar thermal energy source represent a novel innovation in this context. Unlike conventional solar collectors, RTCs harness the thermal absorption of road surfaces, allowing dual functionality of urban spaces, such as sport fields or roads, for both recreational and energy production purposes. This multifunctional design enhances urban spatial efficiency and provides a low-disruption approach to renewable energy harvesting.

One of the key novelties of this work lies in the optimization of system integration. By coupling RTCs with BTES, the study addresses the long-standing challenge of heat production and demand mismatch. The thermal energy harvested by RTCs during the summer is stored in the BTES, which maintains thermal stability over multiple seasons. This approach ensures that heating needs during winter can be met using stored solar energy, thereby significantly reducing reliance on fossil fuels. To our knowledge, the combined use of RTCs, BTES, and water-to-water heat pumps in this specific configuration has not been widely reported in the literature.

The development and validation of a Finite Element Model (FEM) for RTCs, based on experimental data from a real installation at the University of Palermo, is a significant contribution of this work. The FEM was integrated with TRNSYS simulations to provide a comprehensive and dynamic performance analysis of the entire system. This dual-modeling approach enables a more accurate prediction of system behaviour, especially in terms of temperature evolution within the BTES and the energy yields of RTCs.

In terms of environmental contributions, the proposed system aligns with the decarbonization goals of the European Green Deal and has the potential to contribute to broader climate targets. The integration of the proposed system supports the transition to low-carbon heating solutions in the building sector, particularly in educational facilities. However, although this study focuses on a school building, the proposed system configuration can be adapted to other non-residential buildings such as hospitals, offices, and sports complexes. The generalizability of this system design highlights its potential to support low-carbon transitions across a broader range of public and commercial buildings.

Finally, performance metrics, including the Renewable Energy Ratio (RER), Primary Energy Ratio (PER), and Coefficient of Performance (COP), provide a robust framework for evaluating system efficiency and renewable energy integration. The analysis of system stability over an extended operational timeline further highlights the long-term reliability of the proposed system.

Future work could explore optimizing RTC and BTES material, integrating a predictive control algorithm for enhanced efficiency, and adapting the system for colder climate zones.

Materials and methods

This section provides a detailed overview of the proposed system, including the plant configuration and the numerical models developed to simulate the dynamic operation of its components. From this point onward, the system integrating Road Thermal Collectors, Borehole Thermal Energy Storage, and water-to-water heat pumps will be referred to as the Solar and Heat Pump system.

Description of the proposed system: Case study

The Solar and Heat Pump (SHP) system examined in this study integrates a road solar thermal collector with a borehole thermal energy storage system to create a sustainable heating solution. The RTC system harnesses solar energy absorbed by road surface materials in designated urban areas, such as sport fields, converting it into thermal energy. This thermal energy, predominantly produced during the summer months, is stored in the BTES system and later utilised to meet part of the space heating demand of a school building during the winter. The SHP system operates by delivering the stored thermal energy to water-to-water heat pumps, which are powered by electricity supplied by the national grid. This configuration not only leverages renewable energy sources but also enhances overall system efficiency by addressing the seasonal mismatch between energy availability and heating demand.

The school building under consideration is located in Palermo, a city in southern Europe characterized by hot summers, with air temperature values ranging from 19.4 to 35.8 °C, and mild winters, with a minimum air temperature of 4.3 °C [30]. According to Italian regulations, Palermo is classified in climate zone B, with 751 heating degree days (HDD). This classification defines the heating period as extending from December 1st to March 31st, with a maximum of 8 h of heating permitted per day [31].

The school building has a heated volume of 14,500 m^3, and its energy consumption for heating was estimated using a normalisation factor of 13 Wh/m^2 per degree day [32,33].

Fig. 1 shows a schematic overview of the proposed system, highlighting its primary components:

- *RTC system*: Covering approximately 1400 m^2, the RTC comprises four parallel modules, each 4 m wide and 90 m long, equipped with a 16-pipe collector. This area, potentially located around the school and intended for sports activities, retains its original functionality. During periods of high solar radiation, water circulates as the heat transfer fluid through the collectors, absorbing heat and raising its temperature.
- *BTES system*: The BTES system consists of 48 vertical double U-shaped exchangers, each 25 m deep and arranged in concentric circles. This configuration is designed for seasonal thermal energy storage, efficiently retaining heat for use during colder months [34].
- *Heat pump system:* The system includes two water-to-water heat pumps, connected in parallel, with thermal capacities of 200 kW and 300 kW. The evaporators of both heat pumps utilize the BTES system as a low-temperature heat reservoir, extracting heat from the central ring and effectively raising its temperature to meet the thermal requirements of the connected load.
- *Heat exchanger and auxiliary components:* The condensers of the heat pumps are linked to the school's closed-loop heating system via a heat exchanger. This system also incorporates a backup gas boiler to ensure reliability and uses fan coil units for heat distribution within the building.

The sizing of the RTC and BTES systems was defined through a backward energy balance methodology, starting from the school building's seasonal heating demand. The thermal load was estimated using Italian climatic data (751 heating degree days for Palermo) and a normalized consumption factor of 13 Wh/m2·HDD. Based on this load, the heat pump system was dimensioned to operate at a supply

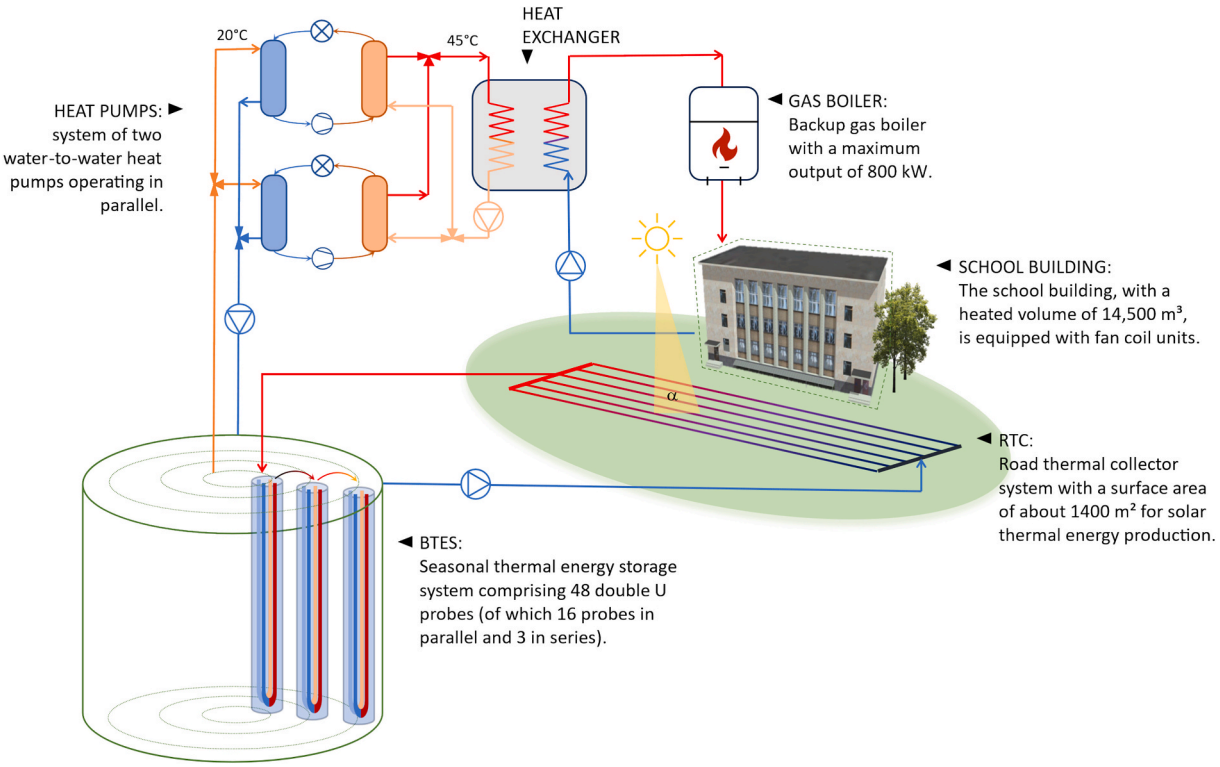

Fig. 1. Schematic representation of the studied integrated renewable energy heating system.

temperature of 45 °C on the load side, with inlet temperatures from the BTES ranging between 8 °C and 20 °C.

To meet these operational conditions, the BTES was designed to store and recover thermal energy with an average temperature differential (ΔT) of 5 °C. Fixing this ΔT and knowing the thermal power required by the evaporators, the total mass flow rate circulating through the BTES during the discharge phase was determined. The number of parallel boreholes in the central ring was then calculated by dividing this total flow rate by the nominal flow rate of a single double-U borehole heat exchanger, assuming fully developed turbulent flow (Re ≈ 10,000). To define the total storage volume—which depends on the volumetric heat capacity of the soil and the target seasonal thermal energy to be stored—the borehole depth and spacing had to be set. While the depth was set at 25 m, a series of simulations was carried out to determine the optimal spacing between boreholes, which in systems of this type typically does not exceed 3 m. The final configuration of 48 boreholes was selected in order to obtain the storage volume required.

The RTC area (1,400 m^2) was sized to provide sufficient thermal input to the BTES during summer charging. This was achieved by scaling a validated experimental RTC module developed and tested at the University of Palermo [28], used here as a modular unit repeated in a series–parallel layout. This modular approach ensures that the thermal energy collected during the summer is well matched to the storage capacity, while maintaining the original function of the area (e.g., playgrounds, paved surfaces) and avoiding additional land use.

In addition to energy balance considerations, the design also ensured hydraulic compatibility between the RTC and BTES circuits. The flow rate circulating in the RTC loop during summer operation was aligned with that of the BTES charging loop, thus enabling efficient heat transfer without imbalance or flow mismatch. This coherence was verified during the simulation setup, where both subsystems were dimensioned to operate within compatible thermal power and flow regimes, ensuring a stable temperature differential and efficient seasonal operation.

This integrated setup combines renewable energy sources with conventional systems, optimizing energy efficiency while providing consistent and dependable heating throughout the year.

Energy model of the solar and heat pump system

The dynamic behaviour of the proposed SHP system was investigated through simulations carried out in TRNSYS environment. The model comprises all the main components of the integrates solar heat pump configuration, allowing detailed performance analysis under realistic boundary conditions. A schematic representation on the TRNSYS layout is reported in Fig. 2, which illustrates the interconnections among the subsystems, control signals, and thermal loops.

To provide a clearer understanding of the operational strategy, Fig. 3 presents a flowchart describing the seasonal control logic that governs the charge/discharge cycle of the integrated system. The flowchart highlights how the system switches from summer to winter operation mode by evaluating specific control conditions. In the heating season (from December to March, in Palermo), the presence of a thermal load triggers the discharge phase of the BTES, with heat being extracted and supplied to the evaporators of the two water-to-water heat pumps. Conversely, during the non-heating season (from April to October, in Palermo), the system switches to the charging phase if all the following conditions are simultaneously met: (i) absence of the heating demand from the building, (ii) the global horizontal irradiance exceeds 150 W/m^2, and (iii) the pipe wall temperature of RTC is equal to or greater than the ambient ai temperature. These criteria ensure that the RTC only operates under favourable solar conditions, maximizing energy harvesting and storage efficiency.

This control logic is implemented in the simulation environment through a binary signal that regulates the activation of the RTC loop. The corresponding activation profile is shown in Fig. 4, where a value of 1 indicates that the circulation pump of the RTC is operating.

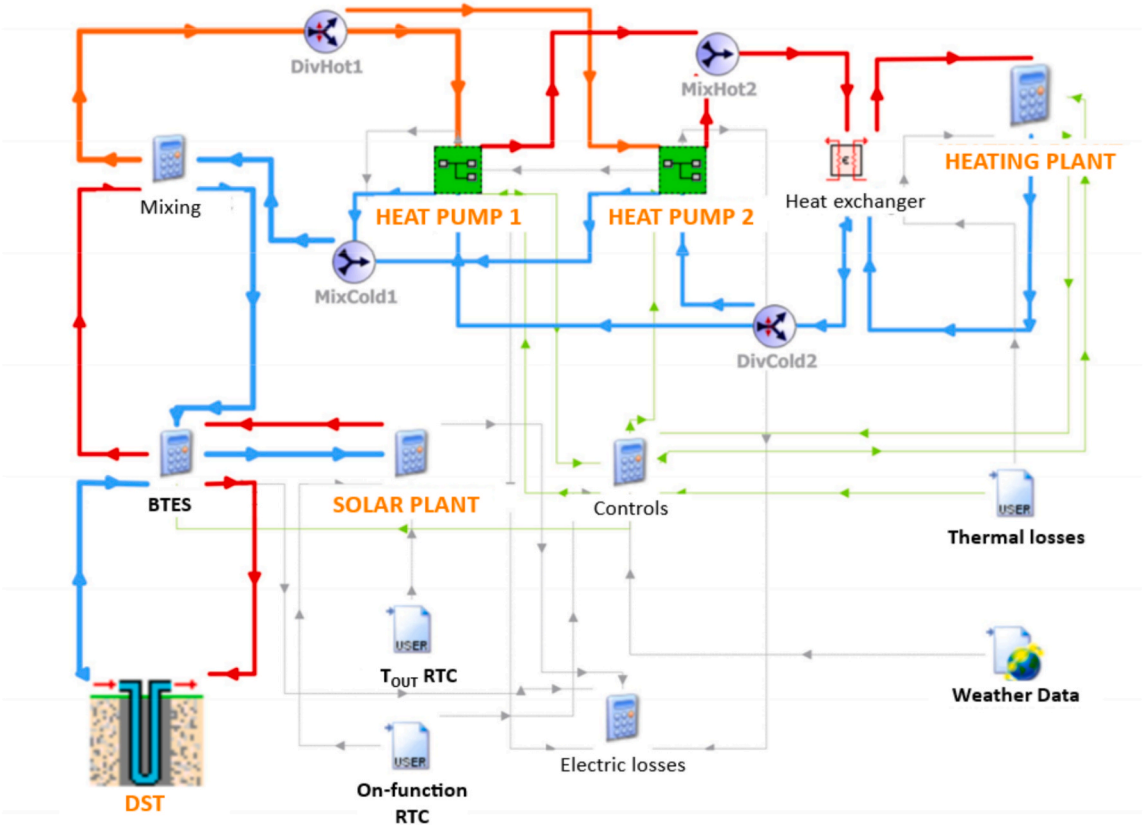

Fig. 2. TRNSYS layout of the proposed system.

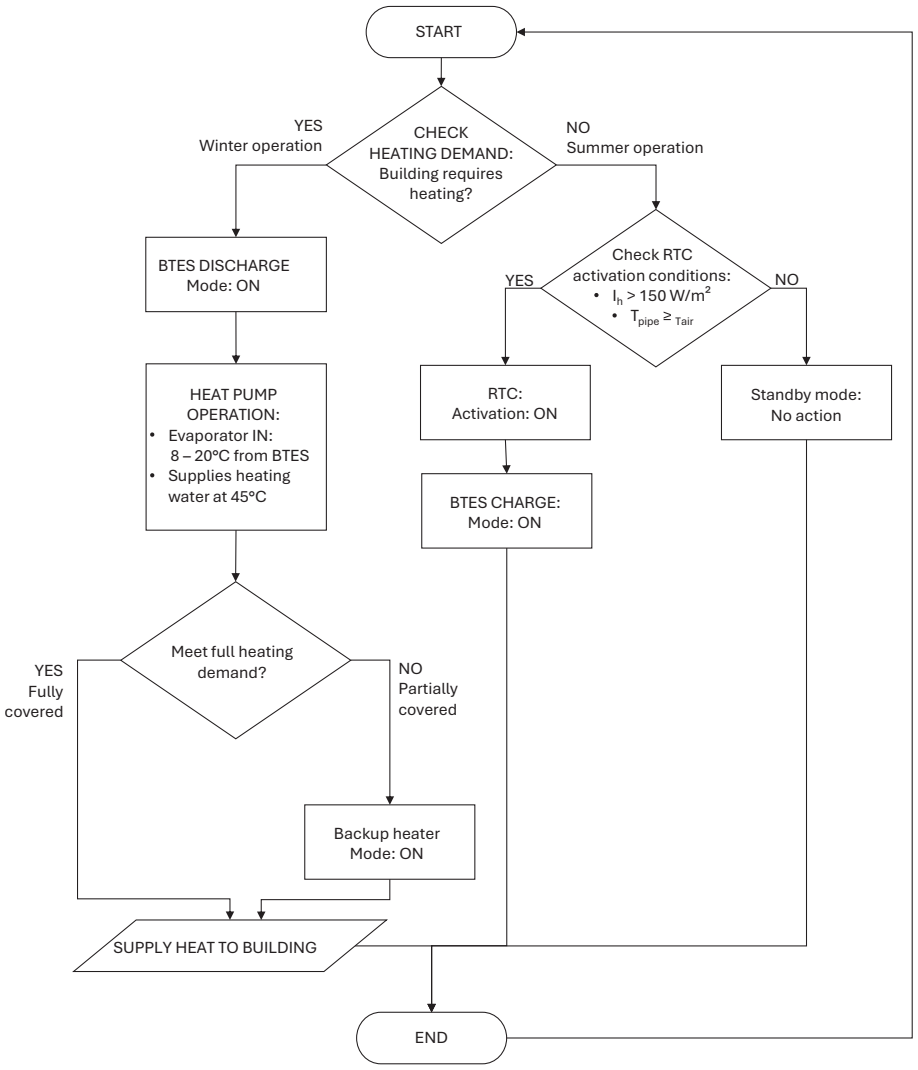

Fig. 3. Detailed flowchart of the SHP system operation, highlighting its seasonal charge/discharge cycle.

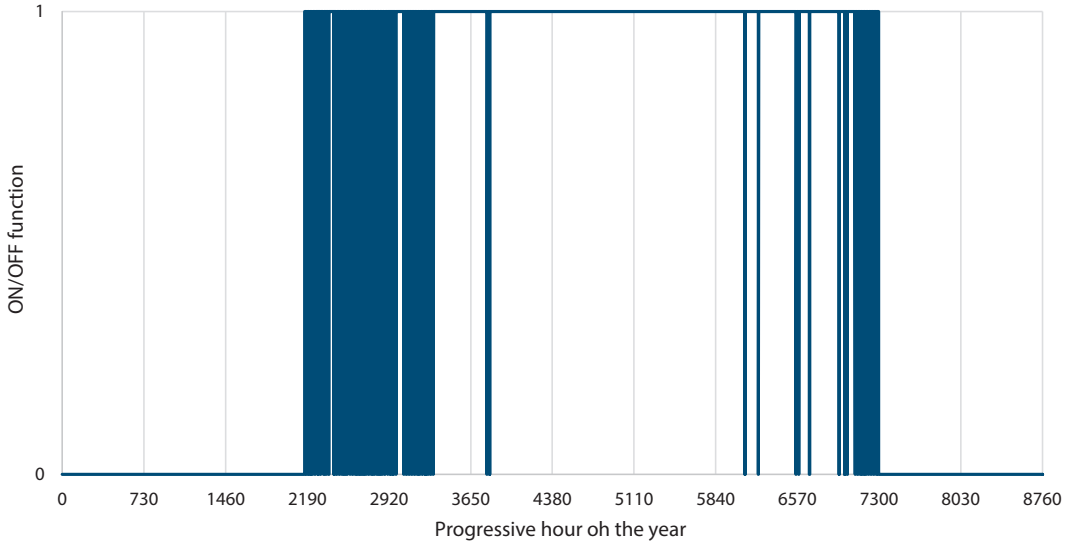

Fig. 4. Binary activation signal of the RTC loop (circulation pump: on = 1; off = 0).

Road thermal collector system model.

A two-dimensional numerical model of the RTC was developed using the Finite Element Method (FEM) to assess its thermal performance. The thermal behaviour of the system is governed by transient heat conduction in the multilayer structure, coupled with surface-atmosphere exchanges and pipe-fluid interactions [28]. The 2D FEM model solves the following transient heat conduction equation:

$$\rho\, c_p \frac{\partial T}{\partial t} = \nabla\cdot(k\nabla T) + G - h_{conv}(T - T_{air}) - \varepsilon\sigma\left(T^4 - T_{sky}^4\right) \quad (1)$$

where:

- ρ, c_p, and k represent the density, specific heat, and thermal conductivity of each material layer,
- G is the absorbed solar irradiance,
- h_{conv} is the convective heat transfer coefficient,
- ε is the surface emissivity, and
- σ is the Stefan-Boltzmann constant.

The top boundary condition accounts for shortwave solar absorption, convective cooling, and longwave radiation, while the fluid pipe-fluid interface is modelled with Newton's law of cooling. The bottom boundary (soil) was assigned a time-dependent sinusoidal temperature profile, derived analytically to reproduce seasonal variation of the ground temperature, as proposed in Buscemi et al. [28]:

$$T(z,\ t) = T_{avg} + A\ \sin\left(\omega t - \sqrt{\omega/2\alpha}\cdot z\right) \quad (2)$$

where, T_{avg} is the average annual ground temperature, A is the amplitude of temperature fluctuation, ω is the angular frequency (annual cycle), z is the depth, and α is the thermal diffusivity of the soil.

The efficiency of the model is influenced significantly by the thermophysical properties of the uppermost layer of the collector and by the energy exchanges at the surface-atmosphere interface. These interactions include solar gains, thermal losses through convection and radiation, and the energy balance of the heat transfer fluid (HTF) flowing inside the embedded pipes. Simulations focused on the transient heat exchange between the HTF and the heat exchanger tubes embedded in the conductive layer. A two-dimensional vertical section was adopted to simplify the geometry while capturing the predominant vertical heat transfer [28].

The FEM model, calibrated and validated using experimental data from an RTC system built in a parking area on the University of Palermo campus, incorporates the geometric and compositional characteristics of the experimental facility. Calibration was based on matching measured and simulated temperature profiles across the layered structure under varying solar and flow conditions. The model showed excellent agreement with experimental data, with a Mean Absolute Error (MAE) of 0.28 °C and a Mean Absolute Percentage Error (MAPE) of 1.7 % for the solid layers of he RTC, as detailed in Buscemi et al. [28]. The simulated outlet temperatures of the heat transfer fluid closely followed the measured temporal trends, with deviations consistently within ± 1.5 °C [28].

Fig. 5 illustrates the three-dimensional schematic of the RTC along with the two-dimensional FEM domain developed in COMSOL Multiphysics®.. The RTC's layered structure consists of an asphalt conglomerate (Layer 1), a conductive concrete layer embedding the pipes (Layer 2), a lightweight/insulating concrete layout (Layer 3), and underlying soil (Layer 4). Detailed dimensions and thermophysical properties are provided in Table 1.

In the numerical model, the thickness of Layer 4 (soil) was set to 3 m. Although the soil extends indefinitely in real-world conditions, a finite domain must be defined in the FEM simulation. The 3-meter depth was chosen to balance computational effort and physical accuracy. At this depth, the soil is not significantly affected by the heat released by the RTC, which is mainly confined to the upper 1–1.5 m. Instead, the temperature fluctuations at this level are primarily driven by seasonal atmospheric variations, modelled through a sinusoidal temperature boundary condition imposed at the bottom of the domain, as described in Equation (2). This approach, commonly adopted in shallow geothermal simulations, allows the representation of realistic thermal dynamics without extending the model to deeper undisturbed zones, which would increase computational complexity without improving the accuracy of near-surface interaction modelling.

The RTC model was integrated with a numerical BTES model, as detailed in the following subsection. Two critical output variables from the RTC model serve as inputs to the BTES model: the outlet temperature of the HTF from the RTC and an on/off control signal to charge the BTES. This integrated multi-physics model enabled dynamic simulations of the system's dynamic response over its first operational year, particularly during the initial thermal loading phase of the BTES. The RTC model provided insights into the collector's thermal production, efficiency, and turn-on/turn-off logic during summer charging periods.

Geothermal energy storage system model.

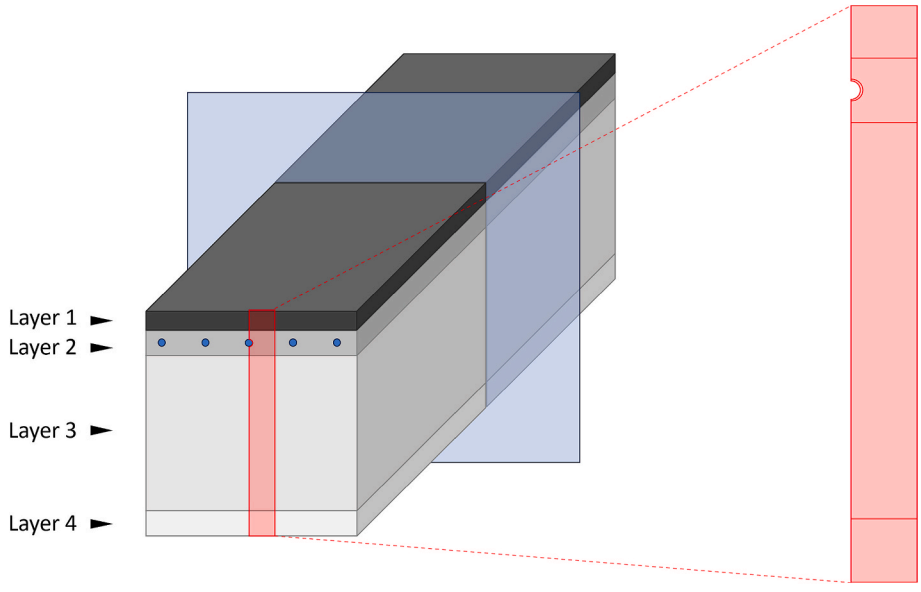

Fig. 5. Schematic representation of the FEM model geometry for the RTC.

Table 1
Geometrical and thermophysical properties of the RTC layers and pipes.

Layer or component	*Material*	*Thermal conductivity*	*Specific heat*	*Density*	*Thickness*	*Inner diameter*
		[W/(m•K)]	*[kJ/(kg•K)]*	*[kg/m^3]*	*[m]*	*[m]*
Layer 1	Asphalt	0.95	1314	1545	0.11	
Layer 2	Conductive concrete	1.828	950	2250	0.07	–
Layer 3	Lightweight concrete	0.948	838	2055	0.5	–
Layer 4	Soil	1.175	1302	1804	3	
Pipe	PeX-A	0.42	2300	932	0.003	0.026

The thermal balance in a BTES system is inherently complex, requiring effective management of energy storage and withdrawal to maintain optimal ground storage temperatures. Excessive storage or withdrawal can reduce system efficiency or lead to long-term degradation [35]. To address these challenges, the TRNSYS Duct Ground Heat Storage Model (DST, *Type 557*) was employed to simulate the transient thermal response of the BTES system. The DST model, originally developed by Hellström [36], enabled the analysis of heat absorption, stored, and recovery processes, while also accounting for heat losses to the surrounding ground at its undisturbed temperature. This model is based on the analytical solution of the transient heat conduction equation in cylindrical coordinates and simulates thermal interaction between multiple vertical boreholes arranged in a grid configuration [36,37]. It assumes radial symmetry and superimposes the thermal responses (g-functions) for multiple boreholes [38]. The governing heat transfer equation solved by the model is:

$$\frac{\partial T(r,\theta,t)}{\partial t} = \alpha\left(\frac{\partial^2 T}{\partial r^2} + \frac{1}{r}\frac{\partial T}{\partial r} + \frac{1}{r^2}\frac{\partial^2 T}{\partial \theta^2}\right) + \frac{q_{in/out}(t)}{\rho c_p} \tag{3}$$

where T is the soil temperature, α is the thermal diffusivity, $q_{in/out}(t)$ is the heat injection or extraction rate per unit of volume, and ρc_p is the volumetric heat capacity of the soil. This equation captures the thermal evolution of the storage field during seasonal operation cycles.

The ground volume affected by heat storage is a function of the total number of probes $(n_{b,t})$, their length (H_b), and the spacing between the concentric rings (s_b) along which these probes are distributed. These parameters can be adjusted to change the geometry of the system and thus optimise the heat storage. The conventional storage volume (V_{BTES}) can be calculated using the following equation:

$$V_{BTES} = \pi \cdot H_b \cdot n_{b,t} \cdot (0.525 \cdot s_b)^2 \tag{4}$$

The geothermal probes that constitute the storage system are arranged in a series–parallel configuration: probes within the central ring are connected in parallel, and each of these is connected in series with probes in progressively outer rings. If $n_{b,h}$ represents the number of probes connected in parallel and $n_{b,s}$ indicates the number of series-connected rings, the total number of boreholes is given by the product of these two parameters in the DST model.

Furthermore, key input parameters for *Type 557* include the undisturbed soil temperature $(T_{s,0})$, thermal conductivities of the pipe (λ_p), grout (λ_g), and soil (λ_s), the heat capacity of the soil $(C_{p,s})$, and the thermal resistance of the borehole (R_p) [39]. These parameters were calibrated using soil properties specific to the Palermo area, ensuring the accuracy of the model [28]. The modelled borehole heat exchangers are double U-tube probes, the cross-section of which is depicted in Fig. 6.

Additionally, optimisation of the proposed BTES system was conducted by running multiple simulations with the DST model. The spacing between boreholes was adjusted while keeping their depth fixed, ensuring the system maintained an optimal thermal balance. This process allowed effective management of energy storage during summer and withdrawal during winter, avoiding overcharging or excessively depleting the system. The choice of relatively shallow boreholes (25 m) was driven by both techno-economic and site-specific geological considerations. In urban environments like Palermo, deeper drilling operations are often constrained by higher costs and regulatory complexity. Additionally, shallow boreholes are sufficient to achieve the desired seasonal thermal storage performance when combined with a solar charging source like the RTC. Although upper soil layers are more exposed to atmospheric variations, the thermal inertia of the system and the continuous summer charging help stabilize the subsurface thermal regime. This depth also avoids interference with underground

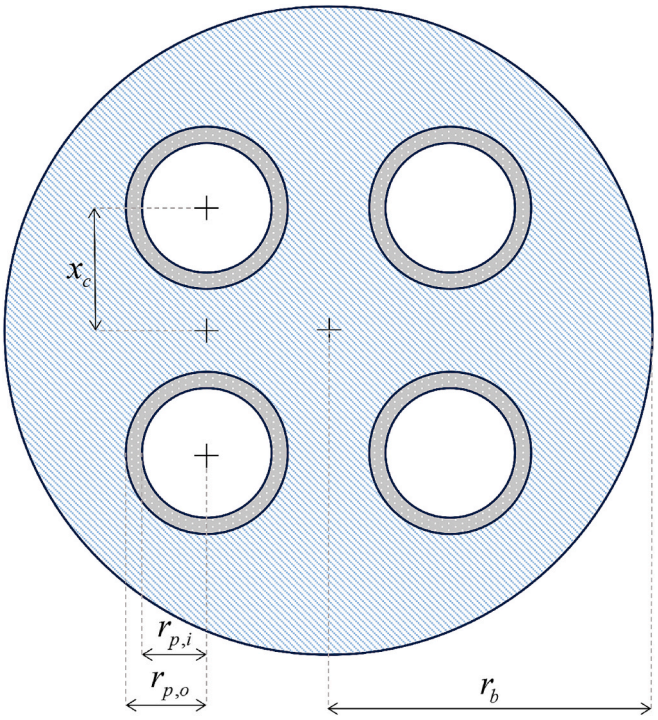

Fig. 6. Cross section of the double U-tube borehole heat exchanger.

Table 2
Parameters of the DST model [40].

Design parameters		
Total number of boreholes,$n_{b,t}$	48	
Number of head boreholes,$n_{b,h}$	16	
Number of boreholes in series,$n_{b,s}$	3	
Borehole depth,H_b	25	m
Spacing between,s_b	3	m
Radius of the borehole, r_b	0.075	m
Inner radius of the pipes,$r_{p,i}$	0.016	m
Outer radius of the pipes,$r_{p,o}$	0.02	m
Half shank spacing between the U-legs,x_c	0.04	m
Thermophysical properties		
Undisturbed Soil temperature,$T_{s,0}$	18	°C
Volumetric heat capacity of the soil,$C_{p,s}$	2.72	GJ/(m^3•K)
Thermal conductivity of the soil,λ_s	1.75	W/(m•K)
Thermal conductivity of the pipe,λ_p	0.45	W/(m•K)
Thermal conductivity of the grout,λ_g	2	W/(m•K)

infrastructure and reduces installation time and costs, making it a viable solution for urban retrofit applications. A summary of the key design parameters is presented in Table 2.

The integration of the DST model was essential for simulating and optimizing the BTES, providing insights into the thermal behaviour of the system under dynamic operating conditions. This process not only enhanced operational efficiency but also ensured the long-term reliability of the BTES within the integrated Solar and Heat Pump system.

To evaluate the seasonal storage performance, the BTES storage efficiency ($\eta_{storage}$) was defined as the ratio between the annual thermal energy extracted from the BTES ($E_{o,BTES}$) and the annual thermal energy injected into it ($E_{i,BTES}$).

$$\eta_{storage} = \frac{E_{o,BTES}}{E_{i,BTES}} \tag{5}$$

These two quantities were obtained from the TRNSYS simulation outputs (*Type 557*), which calculate the transient thermal exchange based on the heat transfer fluid's temperature and flow rate. The integrals of thermal power during charge and discharge phases were post-processed to determine the cumulative energy input and output for each year.

Heat pump system model.

The two water-to-water heat pumps in the system, with thermal outputs of 200 kW and 300 kW, are modelled using a simplified methodology based on manufacturer specifications. Referred to as HP_1 and HP_2, these heat pumps are configured in parallel (Fig. 2). Their operation was evaluated at a condenser outlet temperature of 45 °C, with variable evaporator inlet temperatures ranging from 8 °C to 20 °C (Fig. 7).

The study examined the heat pumps' performance under partial load conditions by analysing their Coefficient of Performance (COP). The Partial Load Ratio (PLR), representing the ratio of the actual thermal load $\left(\dot{Q}_{actual}\right)$ to the heat pump's maximum capacity $\left(\dot{Q}_H^{max}\right)$, was calculated as follows:

$$PLR = \frac{\dot{Q}_{actual}}{\dot{Q}_H^{max}} \tag{6}$$

The Partial Load Factor (PLF) was then determined using the PLR and a nominal COP degradation factor (C_c), which quantifies efficiency losses at partial loads:

$$PLF = \frac{PLR}{C_c \cdot PLR + (1 - C_c)} \tag{7}$$

Then, the actual COP of the heat pump under partial load conditions (COP_{PL}) was calculated by multiplying the nominal COP (the COP at full load – COP_{FL}) by the PLF. The model estimates electricity consumption for both heat pumps under varying operational conditions. The evaporator outlet temperature $(T_{ev,o})$ was calculated as follows:

$$T_{ev,o} = T_{ev,i} - \frac{\dot{Q}_{ev}}{\dot{m}_{f,HP} \cdot c_{p,f}} \tag{8}$$

where $T_{ev,i}$ indicates the inlet evaporator temperature, $\dot{Q}_{ev}$ is the evaporator thermal power of the heat pump, $\dot{m}_{f,HP}$ is the fluid mass flow rate, and $c_{p,f}$ is the specific heat of the fluid. For HP_1 and HP_2, $\dot{m}_{f,HP}$ values were 29,280 kg/h and 48,800 kg/h, respectively.

A control function was integrated into the model to optimize heat pump operation, managing partial loads efficiently in response to hourly thermal energy demand fluctuations. This approach maximizes system efficiency while maintaining reliable performance.

Energy performance metrics

A comprehensive energy analysis was conducted to assess the performance and sustainability of the SHP system. This analysis focused on key performance metrics designed to evaluate the energy efficiency and environmental benefits of the system. The metrics are detailed below:

– *Thermal energy coverage fraction* (f_{HP}): This metric quantifies the fraction of the school's thermal energy demand (E_{load}) met by the heat pump system $(E_{th,HP})$, reducing dependency on conventional energy sources:

$$f_{HP} = \frac{E_{load}}{E_{th,HP}} \tag{9}$$

– *Primary Energy Ratio* (PER): The PER measures the efficiency of converting primary energy into usable heat. It compares the SHP system's primary energy consumption to a reference system that relies solely on a gas boiler. For the SHP system, the PER is defined as

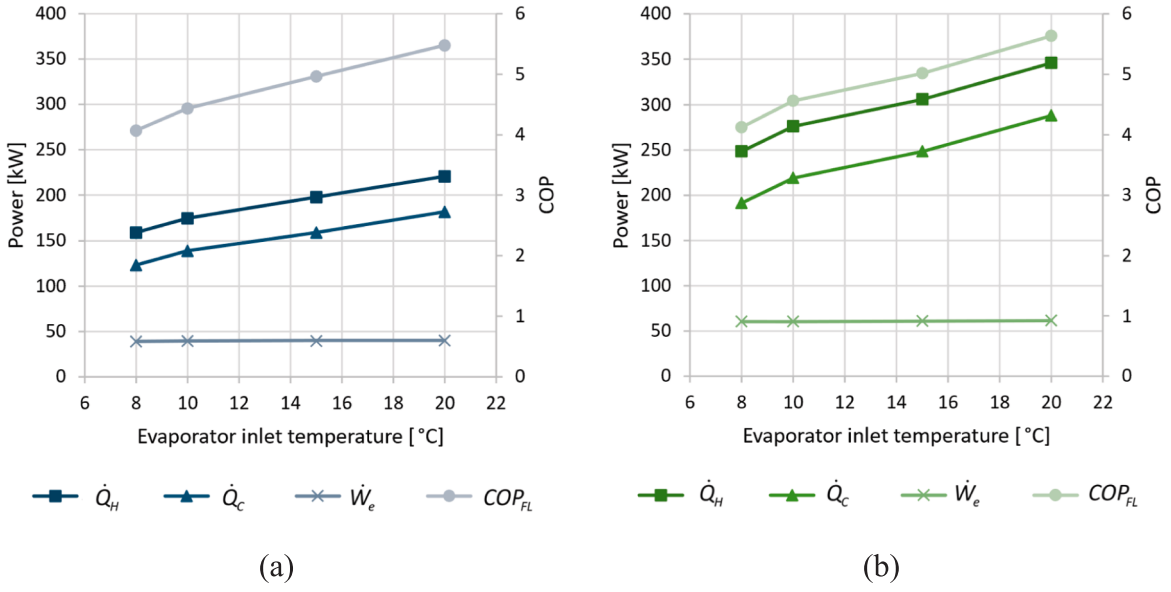

Fig. 7. Operating points of modelled heat pumps for condenser outlet temperature of 45 °C: (a) HP_1 and (b) HP_2.

the ratio between the school's thermal energy demand (E_{load}) and the non-renewable primary energy used as input to the system:

$$PER = \frac{E_{load}}{\frac{E_{boiler} \cdot \varepsilon_{fuel}}{\eta_{boiler}} + E_{e,plant} \cdot \varepsilon_e} \quad (10)$$

Referring to the proposed plant layout, the total primary energy consumption includes both the primary energy required by the plant (for the operation of heat pumps and circulation of the fluid in the RTC and BTES systems) and the primary energy input to the gas boiler, which is used as backup heating system. In Equation (10): E_{boiler} and $E_{e,plant}$ are the annual thermal energy output of the gas boiler and electricity consumption of the plant, respectively; η_{boiler} represents the efficiency of the gas boiler, set at 0.9; ε_{fuel} and ε_e are the primary energy conversion factors for the natural gas and electricity from the grid, respectively, with values of 1.05 kWh_p/kWh_{th} and 1.95 kWh_p/kWh_e [41].

– *Renewable Energy Ratio* (RER): the RER calculates the share of renewable energy contributing to the thermal energy demand:

$$RER = \frac{E_{load}}{E_{ev,HP}} \quad (11)$$

where, $E_{ev,HP}$ represents the annual thermal energy delivered to the heat pump evaporators from the BTES system.

– *Fractional energy savings* (f_{sav}): This metric evaluates the relative energy savings achieved by the SHP system compared to the conventional gas boiler system. It is described by Equation (12):

$$f_{sav} = 1 - \frac{PER_{ref}}{PER_{SHP}} \quad (12)$$

where, PER_{ref} and PER_{SHP} represent the primary energy ratios of the reference gas boiler and SHP systems, respectively. The ratio of these values indicates the relative amount of the non-renewable energy input to the reference system compared to the SHP system.

Environmental indicators

The environmental performance of the SHP system was evaluated by analysing its contribution to reducing carbon emissions compared to a conventional gas boiler system. By utilising solar-generated heat, the SHP system minimizes the dependency on natural gas, which significantly mitigates CO_2 emissions. The annual CO_2 equivalent emissions avoided (C_{eq}) were calculated using the following equation:

$$C_{eq} = \frac{E_{boiler}}{\eta_{boiler}} \cdot \mu_{\substack{natural \\ gas}} + E_{e,plant} \cdot \mu_{\substack{e,fuel \\ mix}} \quad \left[\frac{kg_{CO_{2eq}}}{y}\right] \quad (13)$$

Where:

– E_{boiler} represents the annual thermal energy output from the gas boiler.
– η_{boiler} is the efficiency of the gas boiler (assumed to be 0.9).
– $\mu_{\substack{natural \\ gas}}$ denotes the emission factor for thermal energy produced using natural gas.
– $E_{e,plant}$ is the annual electricity consumption of the SHP system.
– $\mu_{\substack{e,fuel \\ mix}}$ represents the emission factor for electricity from the Italian grid.

In this analysis, the emission factor for thermal energy produced by natural gas combustion is 0.202 $kgCO_{2eq}/kWh_{th}$, while for electricity supplied by the Italian grid, the value adopted is 0.469 $kgCO_{2eq}/kWh_e$ [42,43].

Results and discussion

This section presents the results of the energy and environmental analyses conducted for the proposed Solar and Heat Pump system. The performance of the system was evaluated through dynamic simulations carried out using the numerical model described in the previous section, with a 25-year operational lifetime considered for the analysis.

Energy results

The RTC system operates essentially from April to October, coinciding with periods of high solar energy availability. During these months, the heat transfer fluid circulates through the RTC's embedded pipes whenever the global horizontal irradiance exceeds 150 W/m2 and the pipe wall temperature remains higher than the temperature of the entering fluid. This operation ensures optimal thermal energy collection and transfer to the borehole thermal energy storage system.

Fig. 8 illustrates the thermal dynamics of the RTC system by showing the inlet and outlet temperatures of the HTF, air temperature, and global irradiance values for Palermo. The data correspond to the months from April to October during the 25th year of the system's simulated operation, providing insights into its long-term performance and thermal behaviour.

The analysis reveals that the RTC outlet fluid temperature peaks in July, reaching a maximum value of 43 °C. This highlights the system's ability to harness and transfer significant amounts of thermal energy during periods of high solar radiation. The results underscore the importance of seasonal thermal storage in ensuring that surplus energy collected during summer can effectively meet winter heating demands, reducing reliance on fossil fuels and improving the overall efficiency of the integrated system.

On an annual basis, the RTC system generates a total of 106.4MWh of thermal energy with an average solar-to-thermal conversion efficiency of 5.5 %. To contextualize the performance of the RTC system, a comparison was made with a conventional flat-plate collector (FPC) system. Assuming an average annual solar irradiance of 1,345 kWh/m^2 and a typical thermal efficiency of 50 % for FPCs in Mediterranean climates [44], the equivalent thermal output of 106.4 MWh/year would require approximately 158 m2 of flat-plate collector area. This highlights that the RTC, covering 1,400 m2, is approximately 9 times less efficient in terms of surface-based yield. However, the primary advantage of RTCs does not lie in thermal efficiency, but in their ability to utilize surfaces that are otherwise non-productive from an energy standpoint. By integrating thermal harvesting into existing infrastructure—such as roads, parking areas, and sport fields—RTCs allow for the energetic valorisation of multifunctional urban surfaces, without requiring additional land or compromising the area's primary use. This makes RTCs particularly attractive for densely populated urban contexts where rooftop or open space is scarce or unavailable. Moreover, by extracting heat from paved or asphalted areas during periods of high solar exposure, RTCs may contribute to mitigating the urban heat island effect. This dual benefit—renewable thermal energy generation and local microclimate improvement—reinforces the value of RTCs as sustainable, integrable technologies in the design of climate-resilient cities [29].

Monthly performance metrics illustrate a strong correlation between solar availability and thermal energy output, with the highest energy production observed in July at 23.3 MWh and an efficiency of 6.6 %. In contrast, October recorded the lowest energy output, at 3.2 MWh, with the lowest efficiency. These results highlight the RTC system's ability to harness solar energy effectively, even in Mediterranean climates characterized by high summer temperatures and moderate solar availability during transition seasons.

Table 3 provides a detailed monthly and annual summary of the horizontal solar irradiation (I_h), the solar energy collected by the RTC aperture surface (E_{sun}), thermal energy produced by the RTC system ($E_{th,RTC}$), and the system's monthly efficiency (η_{RTC}) in converting solar

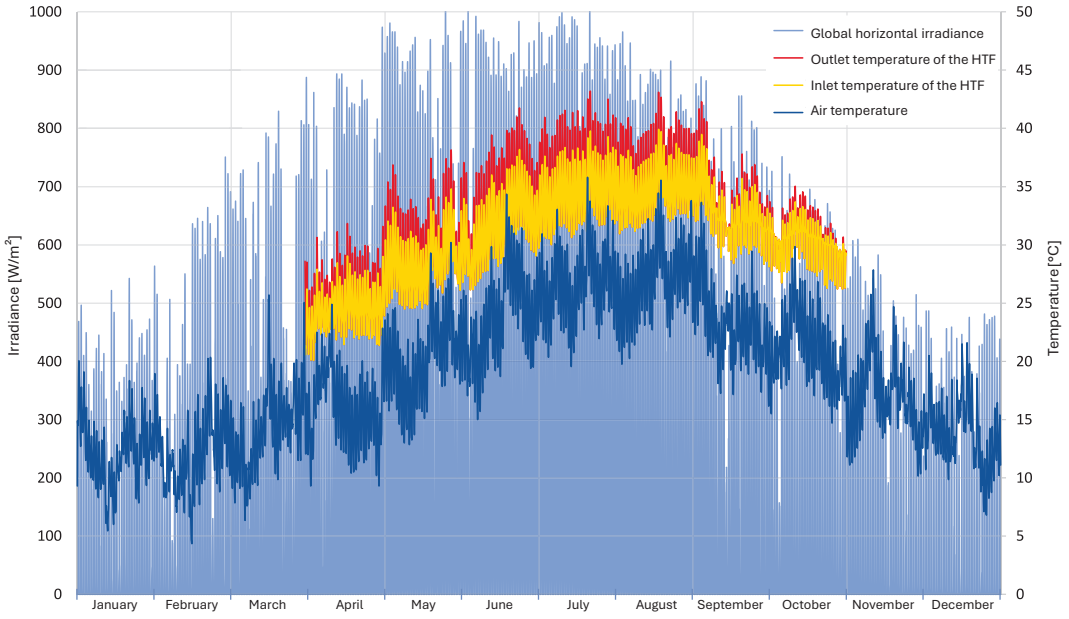

Fig. 8. Simulated inlet and outlet temperatures of the RTC's heat transfer fluid, air temperature, and global solar irradiance from April to October of the 25th year of operation.

Table 3
Monthly and annual cumulative values for solar horizontal irradiation, solar energy collected by the RTC opening surface, thermal energy produced by the RTC, and efficiency.

Month	I_h	E_{sun}	$E_{th,RTC}$	η_{RTC}
	[kWh/m²]	*[MWh]*	*[MWh$_{th}$]*	*[%]*
April	169.1	243.5	12.4	5.1
May	218.7	314.9	19.7	6.3
June	229.0	329.8	22.1	6.7
July	244.9	352.6	23.3	6.6
August	209.9	302.2	17.6	5.8
September	154.6	222.6	8.1	3.6
October	118.8	171.1	3.2	1.8
Annual	**1345.0**	**1936.7**	**106.4**	**5.5**

energy to heat.

The thermal energy produced by the RTC is seasonally stored in the BTES by raising the ground temperature. Fig. 9 depicts the simulated temperatures of the heat transfer fluid at the BTES inlet ($T_{i,BTES}$) and outlet ($T_{o,BTES}$), along with the average storage volume temperature ($T_{ave,BTES}$) between the 24th and 25th years of operation. The alternation between charging (winter months) and discharging periods (summer months) is evident in the temperature trends, reflecting the system's capacity to adapt to seasonal energy demands. The results show that the average storage temperature rises to a peak of 32 °C during the charging phase and subsequently declines to 21 °C at the end of heating season. This dynamic indicates the efficient use of stored energy throughout the year, ensuring a reliable energy supply during demand periods.

Fig. 10 highlights the cumulative energy inputs ($E_{i,BTES}$) and outputs ($E_{o,BTES}$) of the BTES, alongside the average storage temperature over the 25-year simulation. Notably, the system achieves thermal equilibrium by the seventh year of operation, which is crucial for long-term efficiency and stability. On an annual basis, the RTC system supplies 106.4 MWh of thermal energy to the BTES, from which 67.9 MWh are withdrawn by heat pumps. This results in an annual BTES storage efficiency ($\eta_{storage}$) of 63.8 % (see Table 4).

During the school's heating period, the thermal energy stored in the BTES is transferred to two water-to-water heat pumps connected in parallel. The total Coefficient of Performance of the heat pump system is 4.5, while the Seasonal Coefficient of Performance (SCOP), calculated by considering the total electricity consumption of the SHP system, is 4 (see Table 5). This highlights the system's ability to deliver high thermal outputs with minimal electricity input, further enhancing its energy efficiency.

The analysis reveals that the SHP system can meet 0.843 of the school's annual thermal energy demand through the heat provided by the heat pumps. The remaining 17.9 % is supplied by a backup gas boiler, ensuring continuous operation during periods of peak demand or low renewable energy availability.

The performance indicators demonstrate the advantages of the SHP system compared to the conventional gas boiler system, underscoring its effectiveness in integrating renewable energy sources and optimizing energy efficiency. The SHP system achieves a PER of 1.67, significantly exceeding the reference system's 0.86, indicating its superior ability to convert primary energy into useful heat. Similarly, the RER of 1.52 demonstrates the system's effective utilization of renewable energy, with RTCs capturing solar energy and BTES ensuring its availability during colder months. This integration reduces the dependence on fossil fuels and aligns with sustainability goals. Furthermore, the system achieves fractional energy savings (f_{sav}) of 48.6 %, cutting nearly half the primary energy demand compared to the conventional setup. Collectively, these metrics the SHP system's potential as a scalable and sustainable solution for decarbonizing heating in educational and other non-residential buildings, providing a compelling model for achieving energy and environmental targets under real-world conditions.

Environmental results

The environmental analysis reveals a significant reduction in CO_2 equivalent emissions (C_{eq}) when utilizing the SHP system compared to a conventional gas boiler system. \Specifically, the SHP system emits approximately 22.6 tonnes of CO_2 annually, substantially lower than the 37.8 tonnes emitted by the gas boiler reference system. This equates to a reduction of 15.2 tonnes of CO_2 per year, representing a 40.1 % decrease in greenhouse gas emissions. Such results underscore the SHP system's ability to contribute effectively to climate change mitigation efforts.

The lower emissions are attributed to the system's integration of renewable energy sources and advanced energy efficiency measures.

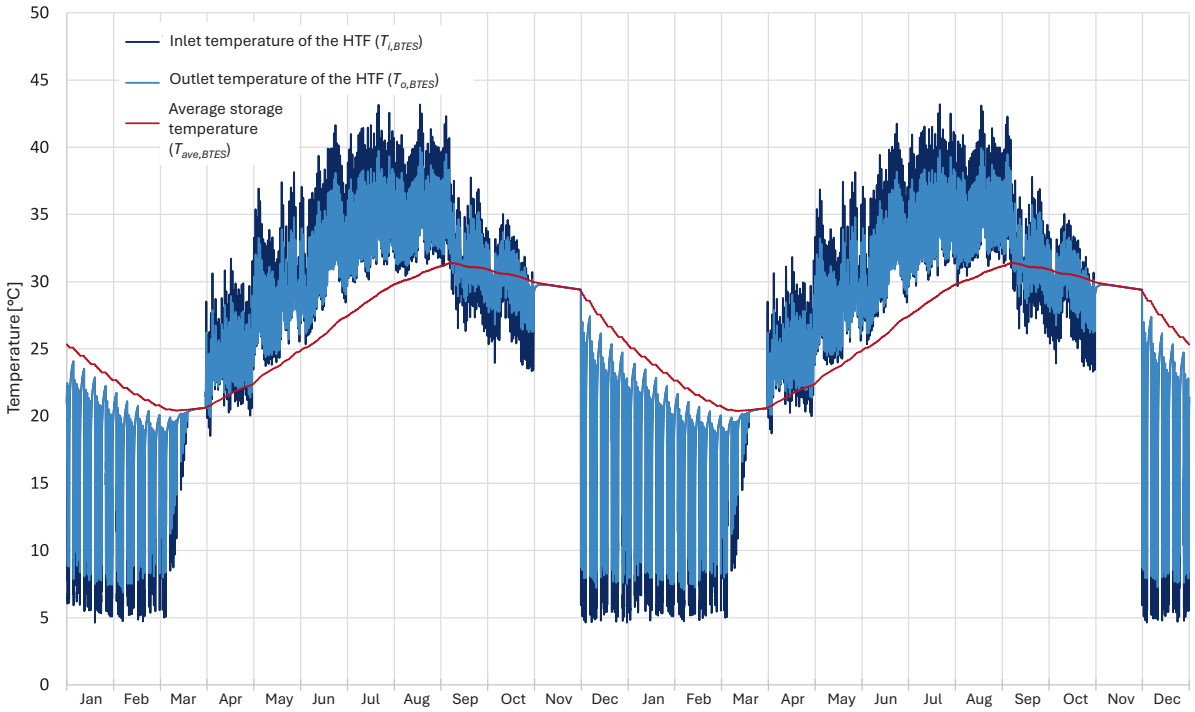

Fig. 9. Simulated temperatures of the heat transfer fluid at the BTES inlet and outlet, along with the average ground temperature in the geothermal storage volume, during the 24th – 25th year of operation.

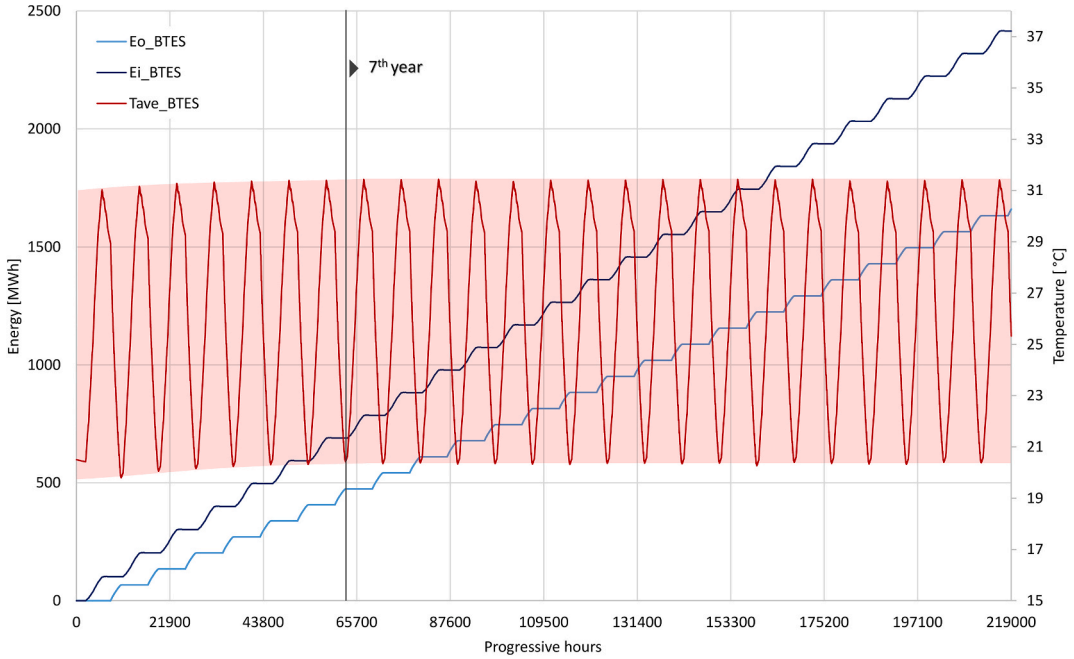

Fig. 10. Cumulative input and output thermal energy values from the BTES, along with the average storage temperature, over the 25-year simulation period.

The SHP system harnesses solar thermal energy through RTCs and stores it seasonally in the BTES, thereby reducing reliance on fossil fuels. This integrated approach not only enhances energy efficiency but also aligns with international decarbonization objectives, such as those outlined in the European Green Deal.

This analysis underscores the SHP system's promise as a scalable and environmentally friendly alternative, paving the way for a more sustainable energy future in the building sector.

Conclusions

This study assessed the performance of a SHP system integrating RTCs for solar thermal energy production, BTES for seasonal heat storage, and water-to-water heat pumps to meet a significant portion of the winter heating demand for a school building in southern Italy. A gas boiler was incorporated as a backup heating system to ensure reliability during peak demand periods.

The results of the analysis revealed several key findings:

Table 4
Monthly aggregate values of thermal energy input and output for the BTES, and the annual efficiency during the 25th year of simulation.

	$E_{i,\ BTES}$	$E_{o,\ BTES}$	$\eta_{storage}$
	[MWh/y]	*[MWh/y]*	*[%]*
January	0.00	20.33	
February	0.00	15.69	
March	0.00	4.31	
April	12.43	0.00	
May	19.75	0.00	
June	22.12	0.00	
July	23.27	0.00	
August	17.62	0.00	
September	8.10	0.00	
October	3.16	0.00	
November	0.00	0.00	
December	0.00	27.59	
Annual	**106.44**	**67.93**	**63.8**

Table 5
Monthly aggregate values of thermal loads, heat supplied by the backup boiler and heat pumps, and electricity consumption of the SHP system.

	E_{load}	E_{boiler}	$E_{th,HP}$	$E_{e,plant}$
	[MWh]	*[MWh]*	*[MWh]*	*[MWh]*
January	59.5	10.6	48.9	11.5
February	38.7	6.3	32.4	8.1
March	6.3	0.1	6.1	2.2
April	0.0	0.0	0.0	0.1
May	0.0	0.0	0.0	0.1
June	0.0	0.0	0.0	0.1
July	0.0	0.0	0.0	0.2
August	0.0	0.0	0.0	0.1
September	0.0	0.0	0.0	0.1
October	0.0	0.0	0.0	0.1
November	0.0	0.0	0.0	0.0
December	62.1	9.2	52.9	12.9
Annual	**166.5**	**26.2**	**140.3**	**35.5**

- The RTC system operates effectively from April to October, leveraging higher solar radiation availability during these months, and achieving an annual efficiency of 5.5 %. Although its conversion efficiency is lower compared to conventional flat-plate solar collectors, RTCs compensate by utilizing multifunctional spaces without compromising their primary function, such as sports areas or road surfaces. The study also identifies the sensitivity of RTC efficiency to higher inlet fluid temperatures from the BTES, underscoring the importance of optimizing RTC configuration (e.g., material properties, layer thickness, and tube spacing) and BTES geometry for enhanced performance.
- The RTC system annually delivered 106.4 MWh of thermal energy to the BTES, raising the average storage volume temperature to approximately 32 °C. The system achieved a seasonal storage efficiency of 63.8 %.
- The heat pump system covered 84.3 % of the total heating load of the school building with a COP of 4.5 and a SCOP of 4, showcasing its ability to efficiently utilize thermal energy.
- The SHP system achieved a PER of 1.67 and an RER of 1.52, resulting in fractional energy savings of 48.9 % compared to a gas boiler-only system. Additionally, the SHP system achieved a 40 % reduction in equivalent CO_2 emissions, aligning with broader decarbonization goals.

The results obtained in terms of energy and environmental performance are comparable with those obtained in the benchmark study [27]. Although the thermal conversion efficiency of RTCs is modest, their integration into multifunctional urban infrastructure enables seasonal energy recovery without additional land use or visual impact, making them particularly suitable for densely built environments. The proposed configuration enabled the system to supply the majority of the building's heating demand with renewable sources while achieving an annual reduction of 15.2 tonnes of CO_{2eq} compared to a conventional gas boiler. These outcomes demonstrate the environmental viability of the solution. Economic assessment was outside the scope of this study and will be addressed in future work. Future developments will also explore a comparative analysis between the proposed solar-assisted RTC–BTES–HP configuration and alternative Ground Source Heat Pump (GSHP) systems without solar charging. In hot climate conditions, where both heating and cooling loads are relevant, this comparison will help assess the seasonal flexibility and economic attractiveness of the two solutions.

In parallel, future work should focus on optimizing the SHP system to enhance its performance and applicability across diverse contexts. Efforts should aim to refine the thermo-physical properties and configurations of RTC and BTES components, ensuring maximum thermal efficiency and storage capacity. Advanced control strategies, such as predictive and adaptive algorithms, could improve system operation under varying climatic and load conditions, reducing reliance on backup heating systems. A detailed economic feasibility analysis is also essential to assess the balance between initial investment costs and long-term operational savings, providing stakeholders with a comprehensive understanding of the system's financial viability. Furthermore, evaluating the SHP system's performance in different climates and expanding its application to other non-residential buildings, such as hospitals and offices, would demonstrate its versatility. Material innovations for RTCs and BTES could further enhance heat transfer, durability, and sustainability, amplifying the system's environmental benefits. These advancements will strengthen the SHP system's role in achieving broader decarbonization targets and support its adoption as a scalable, low-carbon heating solution for the building sector.

CRediT authorship contribution statement

Stefania Guarino: Writing – original draft, Validation, Software, Methodology, Investigation, Formal analysis, Conceptualization. **Alessandro Buscemi:** Validation, Software, Methodology, Formal analysis, Conceptualization. **Marina Bonomolo:** Investigation, Formal analysis, Conceptualization, Validation. **Marco Beccali:** Validation, Supervision, Methodology, Formal analysis, Conceptualization. **Valerio Lo Brano:** Validation, Supervision, Methodology, Formal analysis, Conceptualization.

Declaration of competing interest

The authors declare that they have no known competing financial interests or personal relationships that could have appeared to influence the work reported in this paper.

Acknowledgment

This study was developed in the framework of the research activities carried out within the Project "Network 4 Energy Sustainable Transition — NEST", Spoke 8: Final use optimization, sustainability & resilience in energy supply chain, Project code PE0000021, Concession Decree No. 1561 of 11.10.2022 adopted by Ministero dell'Universita e della Ricerca (MUR), CUP UNIPA B73C22001280006. Project ' funded under the National Recovery and Resilience Plan (NRRP), Mission 4 Component 2 Investment 1.3 - Call for tender No. 341 of 15.03.2022 of Ministero dell'Universita e della Ricerca (MUR); funded by the European ' Union – NextGenerationEU.

Data availability

No data was used for the research described in the article.

References

[1] IEA. Tracking Clean Energy Progress 2023. Paris: 2023.
[2] IEA. World Energy Outlook 2024. Paris: 2024.
[3] UNEP. UNEP's Intergovernmental Council for Buildings and Climate launches at COP29 n.d. https://www.unep.org/technical-highlight/uneps-intergovernmental-council-buildings-and-climate-launches-cop29.
[4] Hafez FS, Sa'di B, Safa-Gamal M, Taufiq-Yap YH, Alrifaey M, Seyedmahmoudian M, et al. Energy Efficiency in Sustainable buildings: a Systematic Review with Taxonomy, challenges, Motivations, Methodological Aspects. Recommendations, and Pathways for Future Research Energy Strateg Rev 2023;45:101013. https://doi.org/10.1016/J.ESR.2022.101013.
[5] Ahmadi M, Piadeh F, Hosseini MR, Zuo J, Kocaturk T. Unraveling building sector carbon mechanisms: Critique and solutions. Renew Sustain Energy Rev 2024;205:114873. https://doi.org/10.1016/J.RSER.2024.114873.
[6] Shaghaghi A, Honarvar F, Jafari M, Solati A, Zahedi R, Taghitahoone M. Thermodynamic and thermoeconomic evaluation of integrated hybrid solar and geothermal power generation cycle. Energy Convers Manag X 2024;23:100685. https://doi.org/10.1016/j.ecmx.2024.100685.
[7] COP28, IRENA, and GRA. Tripling renewable power and doubling energy efficiency by 2030: crucial steps towards 1.5°C. Abu Dhabi: International Renewable Energy Agency 2023.
[8] European Council, Council of the European Union. Fit for 55: making buildings in the EU greener n.d. https://www.consilium.europa.eu/en/infographics/fit-for-55-making-buildings-in-the-eu-greener/#0.
[9] Oke TR. The energetic basis of the urban heat island. Q J R Meteorol Soc 1982;108:1–24.
[10] Mohajerani A, Bakaric J, Jeffrey-Bailey T. The urban heat island effect, its causes, and mitigation, with reference to the thermal properties of asphalt concrete. J Environ Manage 2017;197:522–38.
[11] Nasir DSNM, Pantua CAJ, Zhou B, Vital B, Calautit J, Hughes B. Numerical analysis of an urban road pavement solar collector (U-RPSC) for heat island mitigation: Impact on the urban environment. Renew Energy 2021;164:618–41. https://doi.org/10.1016/j.renene.2020.07.107.
[12] Qin Y. A review on the development of cool pavements to mitigate urban heat island effect. Renew Sustain Energy Rev 2015;52:445–59. https://doi.org/10.1016/J.RSER.2015.07.177.
[13] Bobes-Jesus V, Pascual-Muñoz P, Castro-Fresno D, Rodriguez-Hernandez J. Asphalt solar collectors: a literature review. Appl Energy 2013;102:962–70. https://doi.org/10.1016/j.apenergy.2012.08.050.
[14] Pei J, Guo F, Zhang J, Zhou B, Bi Y, Li R. Review and analysis of energy harvesting technologies in roadway transportation. J Clean Prod 2021;288:125338. https://doi.org/10.1016/J.JCLEPRO.2020.125338.
[15] Hyun SW, Kim S, Jeong H, Ko HS, Shin DH. Development of snow removal system using embedded pipes inside road with solar thermal energy collector and packed bed latent heat thermal energy storage. J Energy Storage 2024;83:110737. https://doi.org/10.1016/J.EST.2024.110737.
[16] IEA. Heating 2023. https://www.iea.org/reports/heating.
[17] Sheng L, Zhang H, Su L, Zhang Z, Zhang H, Li K, et al. Effect analysis on thermal profile management of a cylindrical lithium-ion battery utilizing a cellular liquid cooling jacket. Energy 2021;220:119725. https://doi.org/10.1016/j.energy.2020.119725.
[18] Zhang S, Ocłoń P, Klemeš JJ, Michorczyk P, Pielichowska K, Pielichowski K. Renewable energy systems for building heating, cooling and electricity production with thermal energy storage. Renew Sustain Energy Rev 2022;165:112560. https://doi.org/10.1016/j.rser.2022.112560.
[19] Yang T, Liu W, Kramer GJ, Sun Q. Seasonal thermal energy storage: a techno-economic literature review. Renew Sustain Energy Rev 2021;139:110732. https://doi.org/10.1016/j.rser.2021.110732.
[20] Welsch B, Göllner-Völker L, Schulte DO, Bär K, Sass I, Schebek L. Environmental and economic assessment of borehole thermal energy storage in district heating systems. Appl Energy 2018;216. https://doi.org/10.1016/j.apenergy.2018.02.011.
[21] Sporleder M, Rath M, Ragwitz M. Solar thermal vs. PV with a heat pump: a comparison of different charging technologies for seasonal storage systems in district heating networks. Energy Convers Manag X 2024;22:100564. https://doi.org/10.1016/J.ECMX.2024.100564.
[22] Mohebi P, Roshandel R. Optimal design and operation of solar energy system with heat storage for agricultural greenhouse heating. Energy Convers Manag X 2023;18:100353. https://doi.org/10.1016/J.ECMX.2023.100353.
[23] Falope T, Lao L, Hanak D, Huo D. Hybrid energy system integration and management for solar energy: a review. Energy Convers Manag X 2024;21:100527. https://doi.org/10.1016/J.ECMX.2024.100527.
[24] Simpson JG, Long N, Zhu G. Decarbonized district energy systems: past review and future projections. Energy Convers Manag X 2024;24:100726. https://doi.org/10.1016/j.ecmx.2024.100726.
[25] Lo BV, Orioli A, Ciulla G, Culotta S. Quality of wind speed fi tting distributions for the urban area of Palermo, Italy. Renew Energy 2011;36:1026–39. https://doi.org/10.1016/j.renene.2010.09.009.
[26] Lionello P, Malanotte-Rizzoli P, Boscolo R, Alpert P, Artale V, Li L, et al. The Mediterranean climate: An overview of the main characteristics and issues. In: Lionello P, Malanotte-Rizzoli P, Boscolo R, editors. Mediterranean, vol. 4, Elsevier; 2006, p. 1–DOI: DOI: 10.1016/S1571-9197(06)80003-0.
[27] Panno D, Buscemi A, Beccali M, Chiaruzzi C, Cipriani G, Ciulla G, et al. A solar assisted seasonal borehole thermal energy system for a non-residential building in the Mediterranean area. Sol Energy 2018. https://doi.org/10.1016/J.SOLENER.2018.06.014.
[28] Buscemi A, Beccali M, Guarino S, Lo BV. Coupling a road solar thermal collector and borehole thermal energy storage for building heating: first experimental and numerical results. Energy Convers Manag 2023;291. https://doi.org/10.1016/j.enconman.2023.117279.
[29] Guarino S, Lo Brano V, Kosny J. Understanding the transformative potential of solar thermal technology for urban sustainability. Front Sustain. Cities 2025;7. https://doi.org/10.3389/frsc.2025.1583316.
[30] Meteonorm. Meteonorm - Global meteorological database. Meteotest 2012.
[31] Italian Republic. Decreto del Presidente della Repubblica 26 agosto 1993, n. 412. Italy: Gazzetta Ufficiale; 1993.
[32] Casaccia CR. Guida per il contenimento della spesa energetica nelle scuole. Enea Fire 2008.
[33] Bianchi F, Altomonte M, Cannata ME, Fasano G. Definizione degli indici e livelli di fabbisogno dei vari centri di consumo energetico degli edifici adibiti a scuole-consumi energetici delle scuole primarie e secondarie. ENEA, Rep RSE/2009/119 2009.
[34] Skarphagen H, Banks D, Frengstad BS, Gether H. Design considerations for borehole thermal energy storage (BTES): a review with emphasis on convective heat transfer. Geofluids 2019;2019:4961781.
[35] Xu J, Wang RZ, Li Y. A review of available technologies for seasonal thermal energy storage. Sol Energy 2014;103:610–38. https://doi.org/10.1016/j.solener.2013.06.006.
[36] Hellström G. Ground heat storage 1991.
[37] Hellstrom GAJ. Ground heat storage: thermal analyses of duct storage systems. I Theory 1992.
[38] Yang H, Cui P, Fang Z. Vertical-borehole ground-coupled heat pumps: a review of models and systems. Appl Energy 2010;87:16–27.
[39] Conti P, Testi D, Grassi W. Revised heat transfer modeling of double-U vertical ground-coupled heat exchangers. Appl Therm Eng 2016;106. https://doi.org/10.1016/j.applthermaleng.2016.06.097.
[40] Guarino S, Buscemi A, Ciulla G, Bonomolo M, Lo BV. A dish-stirling solar concentrator coupled to a seasonal thermal energy storage system in the southern mediterranean basin: a cogenerative layout hypothesis. Energy Convers Manag 2020;222:113228. https://doi.org/10.1016/j.enconman.2020.113228.
[41] Famiglietti J, Toosi HA, Dénarié A, Motta M. Developing a new data-driven LCA tool at the urban scale: the case of the energy performance of the building sector. Energy Convers Manag 2022;256:115389. https://doi.org/10.1016/j.enconman.2022.115389.
[42] Our World in Data. Carbon dioxide emissions factors 2023. https://ourworldindata.org/grapher/carbon-dioxide-emissions-factor.
[43] Guarino S, Buscemi A, Messineo A, Lo BV. Energy and environmental assessment of a hybrid dish-stirling concentrating solar power plant. Sustain 2022;14. https://doi.org/10.3390/su14106098.
[44] Weiss W, Spörk-Dür M. Solar Heat Worldwide: Global Market Development and Trends 2022. IEA Sol Heat Cool Program 2023:88.